GEOFIZIKA VOL. 40 2023

DOI: https://doi.org/10.15233/gfz.2023.40.8
Original scientific paper

Mediterranean meteotsunamis of May 2021 and June 2022: Observations, data analysis and synoptic background

Mia Pupić Vurilj [1, 2], *Tina Brnas* [2], *Krešimir Ruić* [2], *Jadranka Šepić* [2] *and Marijana Balić* [2]

[1] Faculty of Civil Engineering and Geosciences, Delft University of Technology, Delft, Netherlands

[2] Faculty of Science, University of Split, Split, Croatia

Received 10 January 2023, in final form 2 October 2023

Meteorological tsunamis (*i.e.*, tsunami-like waves of atmospheric origin) are regularly observed in the Mediterranean Sea. During a single event, destructive flooding usually occurs in one location or limited area. However, in May 2021 and June 2022, strong meteotsunamis hit several Mediterranean locations up to 500 km apart. In the morning hours of the 24th of May 2021, a meteotsunami hit Bonifacio on the island of Corsica (western Mediterranean, France) and in the afternoon hours of the same day, another meteotsunami hit Široka Bay on the island of Ist (Adriatic Sea, Croatia), 500 km away. About 13 months later, on the 26th of June 2022, a meteotsunami hit Ciutadella on the island of Menorca (Spain) and two days later Bonifacio, 400 km away. Sea-level and atmospheric pressure data and satellite imagery, as well as synoptic conditions, associated with both events were analysed in detail. It has been confirmed that in the Mediterranean, meteotsunamis occur when meteotsunamigenic synoptic conditions prevail over the area, with a strong southwesterly jet stream embedded in dynamically or convectively unstable atmospheric layers standing out as the most important condition. The meteotsunamigenic potential of each of the three bays (Ciutadella, Bonifacio, Široka Bay) was investigated by considering: (1) the potential for Proudman resonance on the shelves offshore of the bays, (2) the orientation of the mouth of the bay and (3) the frequency of meteotsunamigenic synoptic conditions over the area. The strongest and most frequent meteotsunamis occur at locations where the shelf characteristics (width, depth, orientation), bay mouth orientation and climatology of 500-hPa winds and atmospheric stability have characteristics that support the amplification of long-ocean waves and their propagation toward the bay mouth.

Keywords: meteotsunami, Mediterranean Sea, Adriatic Sea, extreme sea-levels, high-frequency sea-level oscillations, Proudman resonance

1. Introduction

On the 24th of May 2021, Bonifacio on the island of Corsica (western Mediterranean Sea, France) and Široka Bay on the island of Ist (Adriatic Sea, Croatia) were hit by damaging tsunami-like waves (Fig. 1). Bonifacio was suddenly flooded by ~1 m high waves in the morning hours (Fig. 2; corse matin, 2021; Centro Meteo Italiano, 2021) and a similar incident occurred later in the day in Široka Bay. In Široka Bay, according to eyewitness accounts, the sea initially retreated causing some boats to fall to the seabed (Fig. 2) and then, after a few minutes, rose to ~1–1.5 meters above pre-event level causing significant property damage and flooding. According to a field survey, the height of sea-level oscillations in Široka Bay was estimated to be 2–3 m (Šepić and Orlić, 2023).

About a year later, on the 26th of June 2022, 0.95 m tsunami-like waves were recorded in Ciutadella (Balearic Islands, Spain) (Menorca, 2022) and on the 28th

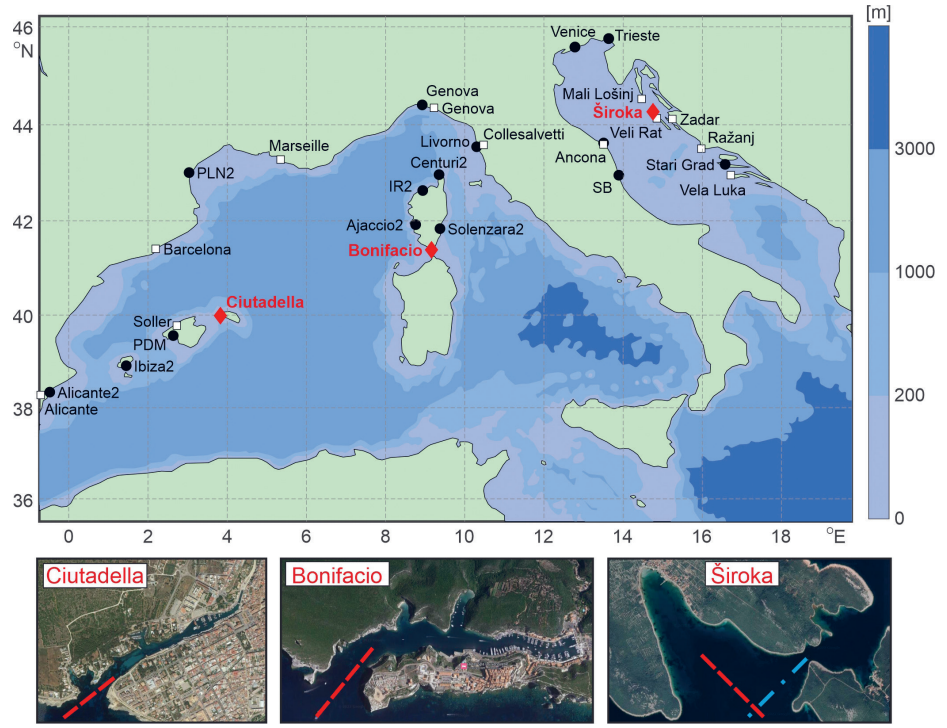

Figure 1. (*upper*) Map of the western Mediterranean and Adriatic Sea. Places hit by meteotsunamis are marked with red diamonds. Black circles mark tide gauge stations and white squares air pressure stations. "PDM" stands for Palma de Mallorca; "PLN" for Port la Novuelle; "IR" for Ille Rousse; "SB" for San Benedetto del Tronto. (*bottom left*) Ciutadella; (*bottom middle*) Bonifacio; (*bottom right*) Široka Bay. The red dashed lines in the lower plots are oriented to the harbour/bay entrances; the blue dot-dashed line is oriented towards the narrow strait between Ist Island and Molat island – the lines correspond to orientations indicated in Fig. 13. Satellite images were taken from Google Maps (https://www.google.com/maps).

of June, at noon local time, Bonifacio was also flooded by similar waves (corse matin, 2022). Široka Bay (Ist) was not affected this time. We will show that the May 2021 and June 2022 events were meteorological tsunamis and that their successive occurrence over more than 500 km distance was related to the northeastward propagation of a meteotsunamigenic synoptic system over the western Mediterranean and Adriatic Seas.

Meteorological tsunamis or meteotsunamis are long-ocean waves that have temporal and spatial dimensions of seismic tsunamis but are generated by atmospheric processes *i.e.*, by intense atmospheric pressure disturbances (Monserrat et al., 2006). These disturbances are associated with atmospheric gravity waves, convective pressure jumps, frontal lines and gusts (Hibiya and Kajiura, 1982; Rabinovich and Monserrat, 1996; Monserrat et al., 2006; Rabinovich, 2009). Over the open ocean, atmospheric pressure disturbances generate long-ocean waves that can be amplified by resonance mechanisms. Possible resonances include Proudman resonance (when the translational speed of the atmospheric disturbance is equal to the longwave speed of the ocean waves; Proudman, 1929), Greenspan resonance (when the alongshore component of the atmospheric disturbance velocity is equal to the speed of one of the modes of the edge waves; Greenspan, 1956) and the shelf resonance (when the atmospheric disturbance and the generated ocean wave have periods and/or wavelengths equal to the resonant period and/or wavelength of the shelf region) (Monserrat et al., 2006). The above-mentioned resonances can result in a tenfold increase in wave height (*e.g.*, from 3–4 cm to 30–40 cm). Upon approaching the coast, the long-ocean waves further increase due to the shoaling effect (Green's law; Lamb, 1932). Meteotsunami waves can reach potentially dangerous heights both on the open coast (*e.g.*, Daytona Beach, Florida, Sallanger et al., 1995 and Rabinovich, 2020; Odessa, Black Sea, Šepić et al., 2018a; Mostaganem, Algeria, Okal, 2021) and in bays with strong resonant properties (*e.g.*, Nagasaki Bay, Hibiya and Kajiura, 1982; Ciutadella, Balearic Islands, Jansà and Ramis, 2021; Vela Luka, Adriatic Sea,

Figure 2. Stranded boats in Ist (Dnevnik.hr, 2021) (*left*); flooding in Bonifacio (corse matin, 2021) (*right*), both during the May 2021 events.

Vučetić et al., 2009; Orlić et al., 2010). In such bays, long-ocean waves are further amplified due to harbour resonance and narrowing and shoaling effects. Harbour resonance occurs when the period of incoming long-ocean waves coincides with the period of eigen-oscillations of a bay (harbour) (Raichlen, 1966). In addition to flooding, meteotsunamis are also associated with strong currents that are a danger to infrastructure (Fremantle, Australia, Pattiaratchi and Wijeratne, 2015) and potentially fatal for swimmers (Great Lakes, USA, Linares et al., 2019).

Before going further, we note that meteotsunamis are defined differently in different literature sources. Some authors set a specific sea-level height as the threshold for a meteotsunami over the entire area of interest (*e.g.*, 1 m in the Adriatic meteotsunami catalogue; Orlić, 2015; Šepić and Orlić, 2023). Other authors define a station-dependent threshold based either on percentiles of wave height (*e.g.*, Pellikka et al., 2022) or on a critical wave height (*e.g.*, Rabinovich and Monserrat, 1996; Šepić et al., 2009a). Following Orlić (2015) and Šepić and Orlić (2023), we choose a fixed threshold of ~1 m height to define a meteotsunami. In addition, we refer to smaller, but apparent, short-period ($T < 2$ h) sea-level oscillations, as "intensified high-frequency oscillations".

Many bays and harbours of the Mediterranean are prone to meteotsunamis. In Ciutadella (Balearic Islands), meteotsunamis are known by the local name "rissaga" (Jansà and Ramis, 2021). Waves of ~1 m height occur there a few times per year and destructive rissagas with wave heights greater than 2 m once every 4–5 years (Monserrat et al., 2006). The strongest events in the last 40 years happened on the 21st of June 1984 (Jansà and Ramis, 2021) and on the 15th of June 2006 (Jansà et al., 2007; Vilibić et al., 2008). Meteotsunamis are also a common phenomenon in the Adriatic Sea where they are known as "šćiga" (Vilibić and Šepić, 2009; Vilibić et al., 2021; Šepić and Orlić, 2023). The best-known Adriatic meteotsunami hotspot is Vela Luka (Korčula Island), where, among other events, the great Vela Luka flood of the 21st of June 1978 occurred. During this event, the inner bay was flooded by ~6-meter-high waves of ~15–20 min period (Orlić, 1980; Vučetić et al., 2009; Orlić et al., 2010). Another location in the Adriatic where strong meteotsunamis occur is Široka Bay on the island of Ist. In the last 40 years and prior to the 24th of May 2021 event, two strong meteotsunamis hit Široka Bay (on October 5th 1984 and on August 22nd 2007, the wave heights of oscillations were ~4 m in both events; Šepić et al., 2009b; Šepić and Orlić, 2023). Prior to 2021, we were not aware of meteotsunamis in Bonifacio Bay. Nonetheless, an extensive web search revealed that tsunami-like waves of unknown strength occasionally happen there. "Jf84", a forum user, (https://www.hisse-et-oh.com/sailing/phenomene-de-maree-etonnant-a-bonifacio) describes a probable meteotsunami in June 2007 "… it reminds me of something seen in Bonifacio in June 2007. Between 6 a.m. and 8:30/9 a.m., I observed a very curious tidal phenomenon, the water dropped by around 1 m in 10–15 min only to return and rise by the same amount (*i.e.*, almost 2 m of tidal range) in an equivalent time. This

phenomenon repeated itself 3 or 4 times before disappearing. The water was rising to the bars along the harbour. … Amel (sailing ship) engaged its bow under the pontoon when it went down and found itself stuck under the pontoon when the water returned, for example... The locals did not seem surprised, a visibly recurrent phenomenon." The additional two Mediterranean meteotsunami hotspots are the Maltese coast (local name "milghuba", Drago, 1999) and Mazara del Vallo in Sicily (local name "marrobbio"; Candela et al., 1999; Šepić et al., 2015a; Šepić et al., 2018b; ; Zemunik et al., 2020).

During a single event/date, meteotsunamis usually manifest as destructive flooding in a single area, *i.e.*, a bay or a limited section of coastline. However, successive meteotsunamis can occur over much larger areas. One of the best-known examples was the Mediterranean and Black Seas meteotsunami chain of 23rd to the 27th of June 2014 (Šepić et al., 2015a): a moderate meteotsunami (~1 m) was first observed in Ciutadella (23rd of June), then a few days later much stronger meteotsunamis in numerous bays in the Adriatic Sea (25th and 26th of June; maximum wave heights up to ~3 m, Šepić et al., 2016) and in Mazara del Vallo in Sicily (25th of June; tsunami bore; Šepić et al., 2018b). Finally, strong meteotsunami waves hit Odessa, Ukraine, on the 27th of June (Šepić et al., 2018a). The June 2014 meteotsunamis were triggered by numerous mesoscale (O(10–100 km)), short-lived (up to a few hours) atmospheric pressure disturbances generated continuously from the 23rd to the 27th of June 2014. The generation of these atmospheric disturbances was supported by a meteotsunamigenic synoptic system that propagated from the western to the eastern Mediterranean Sea over a period of seven days (Šepić et al., 2015a).

Over the Mediterranean, meteotsunamigenic synoptic conditions are associated with a Rossby wave that is clearly visible at a level of 500 hPa (*e.g.*, Fig. 3 in Šepić et al., 2015a), with meteotsunamis occurring at the front of its trough. Such a wave supports: (i) a surface pressure low to the west of the area affected by a meteotsunami; (ii) an inflow of warm and dry African air at an altitude of ~ 850 hPa; (iii) a strong southwesterly wind at a level of ~ 500 hPa; and (iv) a presence of unstable atmospheric layers (at altitudes of ~ 500 hPa), identifiable by a small Richardson number, $Ri < 0.25$ (Šepić et al., 2015a), where (ii)-(iv) are usually found directly over the area hit by a meteotsunami.

These conditions, of which some were recognised as meteotsunami favourable in early studies of the Ciutadella and Adriatic events (Hodžić, 1979/1980; Ramis and Jansà, 1983), support formation and propagation of pronounced atmospheric pressure disturbances (*e.g.*, Monserrat and Thorpe, 1996). The first study to estimate the meteotsunamigenic effect of the propagation of such a synoptic system from one Mediterranean region to another was conducted by Šepić et al. (2009a). In their work, the authors compared the simultaneous occurrence of meteotsunamis in Ciutadella and Dubrovnik (Adriatic Sea, Croatia) in the period 1975–1998. The authors showed that 16 out of 32 Ciutadella meteotsunamis (Ciutadella meteotsunami was defined as an event with a wave height > 0.4 m) were followed within 1–2 days by a meteotsunami in Dubrovnik (Dubrovnik

meteotsunami was defined as an event with a wave height > 0.05 m). It was shown that meteotsunamis are most likely to occur at both locations when meteotsunamigenic synoptic conditions propagate from the Balearic Islands to the Adriatic Sea. Instability of the upper atmospheric layers was the most persistant synoptic condition: mid-tropospheric atmospheric layers were unstable in 31 of 32 Ciutadella meteotsunamis and in all 16 of Dubrovnik meteotsunamis.

Later, Šepić et al. (2015b) extended the study to a larger area, this time using 1-min sea-level data from 29 Mediterranean sea-level stations evenly distributed from the western to the eastern Mediterranean Sea (but excluding the Adriatic Sea, as no 1-min data of long enough duration were publicly available at the time). The conclusion was the same: intensified high-frequency sea-level oscillations occurred successively over different parts of the Mediterranean Sea following the propagation of a common synoptic pattern.

As noted already, successive meteotsunamis (or intensifications of high-frequency sea-level oscillations) over the Mediterranean Sea are caused by continuously generated atmospheric pressure disturbances (Šepić et al., 2015a). However, there are also situations where a single long-lasting atmospheric pressure disturbance propagating over hundreds to thousands of kilometres causes consecutive meteotsunamis (or intensified high-frequency oscillations) (Šepić and Rabinovich, 2014). A recent study by Zemunik et al. (2022), which utilized global sea-level data but did not include a detailed analysis of synoptic conditions, found a 20–32% probability of simultaneous intensification of high-frequency sea-level activity over distances of up to 250 km in mid-latitudes.

In this manuscript, we analyse May 2021 and June 2022 meteotsunami events in the Mediterranean Sea, providing a detailed analysis of oceanic and atmospheric in-situ data, satellite data and reanalysis data. We also analyse the background reasons that lead to some locations being considered meteotsunami hotspots. Section 2 presents material and methods, Section 3 analyses the 2021 event and Section 4 analyses the 2022 event. The manuscript ends with a discussion (Section 5) and conclusions in Section 6.

2. Materials and methods

Sea-level data of 1-min time resolution were downloaded from the Intergovernmental Oceanographic Commission (IOC) of UNESCO (https://www.ioc-sealevelmonitoring.org/) for all available tide gauges of the western Mediterranean and Adriatic Sea for the entire period of availability. In addition, the Ciutadella sea-level data for the June 2022 event were downloaded from the Joint Research Center (JRC) TAD SERVER website (https://webcritech.jrc.ec.europa.eu/TAD_server/Device/125). The Ciutadella JRC TAD data were available with a variable temporal resolution (median of 2.1 min) and were interpolated to a 1-min time step prior to analysis. Sea-level data were high-pass filtered using a 2-h Kai-

ser-Bessel filter (*e.g.*, Thomson and Emery, 2014). The filtered sea-level series with a length of more than 1 year were further analysed as follows (for each available station separately): (1) the series were divided into 2-h intervals; (2) for each of these 2-h intervals, the wave heights of all oscillations were estimated; (3) a new time series "*2-h wave height maxima*" was created consisting of the maximum wave heights of all 2-h intervals. Sea-level oscillations recorded during the May 2021 and June 2022 events were compared to the "*2-h wave height maxima*" series to determine how intense the event oscillations were when compared to background oscillations at each station, *i.e.*, their percentile compared to the "*2-h wave height maxima*" series were determined.

Atmospheric pressure data were obtained from three data providers. The Adriatic data for Zadar, Veli Rat and Mali Lošinj had a time resolution of 10-min and were obtained from the Croatian Meteorological and Hydrological Service (https://meteo.hr/). Data for the other three stations in the Adriatic (Vela Luka, Ražanj and Ancona) had a time resolution of 1-min and were downloaded from the Institute of Oceanography and Fisheries (Split) website (http://faust.izor.hr/autodatapub/postaje2). Atmospheric data from stations in the western Mediterranean (Alicante, Barcelona, Soller, Marseille, Genova and Collesalvetti) had a time resolution of 2-min and were downloaded from the Sensor Community website (https://sensor.community/en/). The Sensor community data must be downloaded day-by-day from the website https://archive.sensor.community/. All atmospheric data were high-pass filtered using a 2-h Kasier-Bessel window.

Satellite images were downloaded from the EUMETSAT website (https://www.eumetsat.int/). Two types of satellite images were downloaded: (1) high-rate SEVIRI infrared (IR) imagery at 10.8 μm and (2) processed convection RGB channel imagery.

Data from the ERA5 global reanalysis (Hersbach et al., 2020; Copernicus Climate Change Service (C3S), 2017) were used to evaluate synoptic conditions during the May 2021 and June 2022 events. We examined hourly fields of: (1) mean sea-level pressure; (2) temperature at 850 hPa; and (3) wind and geopotential height at 500 hPa. We also calculated the Richardson number (*Ri*), an index of atmospheric stability, as follows:

$$Ri = \frac{N^2}{(d\left|\vec{U}\right| / dz)^2} \tag{1}$$

where, N is the Brunt-Väisälä frequency, $\left|\vec{U}\right|$ is the wind speed and z is the vertical distance between layers. The Brunt-Väisälä frequency (N) was calculated according to Durran and Klemp (1982), using the moist Brunt-Väisälä frequency expression for levels where relative humidity was above 70% (*e.g.*, Šepić et al., 2015a) – otherwise the dry Brunt-Väisälä frequency expression was used. The Richardson number was estimated for levels from 600 to 400 hPa. For the ERA5 times closest to times of meteotsunamis occurrences, the Froude number was estimated as follows:

$$Fr = \frac{\sqrt{u_{500}^2 + v_{500}^2}}{\sqrt{gh}} \tag{2}$$

where u_{500} and v_{500} are the ERA5 wind components at 500 hPa, g is the gravity acceleration and h is the ocean depth. To calculate the Froude number, the ERA5 wind variables (0.25° × 0.25°) were interpolated onto the ocean bathymetry grid (0.0042° × 0.0042°). Ocean bathymetry was downloaded from the GEBCO website (https://download.gebco.net/; Weatherall et al., 2015). The ERA5 data were also used to determine the general climatology of mid-tropospheric winds (500 hPa) and atmospheric stability (600–400 hPa) during May to November, being the period when meteotsunamis are most common in the Mediterranean Sea, for the 30-year period from 1993 to 2022.

Following Šepić et al. (2016), we estimated the Proudman length for Ciutadella, Bonifacio and Široka Bay. Proudman length (*PL*) is a variable that indicates the potential of the shelf to support the generation of long-ocean waves by Proudman resonance and can be defined as follows:

$$PL = \frac{L_{Fr\_crit}}{L_{tot}} \tag{3}$$

where L_{Fr_crit} is the length of path over which the Froude number (Fr) is within the range $0.7 < Fr < 1.3$ and L_{tot} is the total path length spanning off the point of interest towards a selected direction. The Proudman length was estimated for a hypothetical atmospheric disturbance coming from angles of 0° to 355° (with a gradation of 5°) and for speeds of 10 to 50 m/s (with a gradation of 1 m/s) and propagating over a fixed length of 150 km. It should be noted that the limits for Fr are somewhat relaxed (following the here presented analyses) compared to the ones used by Šepić et al. (2016) and Pellikka et al. (2022), where the Proudman lengths were estimated for $0.95 < Fr < 1.05$.

3. Meteotsunamis of May 2021

High-frequency sea-level data recorded from the 23rd to the 26th of May 2021 are shown in Fig. 3. The stations are ordered from southwest to northeast, with the Solenzara tide gauge closest to Bonifacio (~60 km distance) and the Ancona tide gauge (~125 km distance) closest to Široka Bay. Enhanced high-frequency sea-level oscillations were detected at all tide gauges in the western Mediterranean and Adriatic Seas: first at the southwestern stations during the midday and afternoon hours of the 23rd of May (Alicante2, Ibiza2, Palma de Mallorca, Ciutadella), then during the morning and midday hours of the 24th of May in Corsica and on the French and Italian Mediterranean coasts (Port la Novuelle to Livorno) and finally during the afternoon hours of the 24th of May at the Adriatic stations. The onset of oscillations at the tide gauge stations closest to Bonifacio and Široka Bay coincides with the times of observed tsunami-like waves at these two stations.

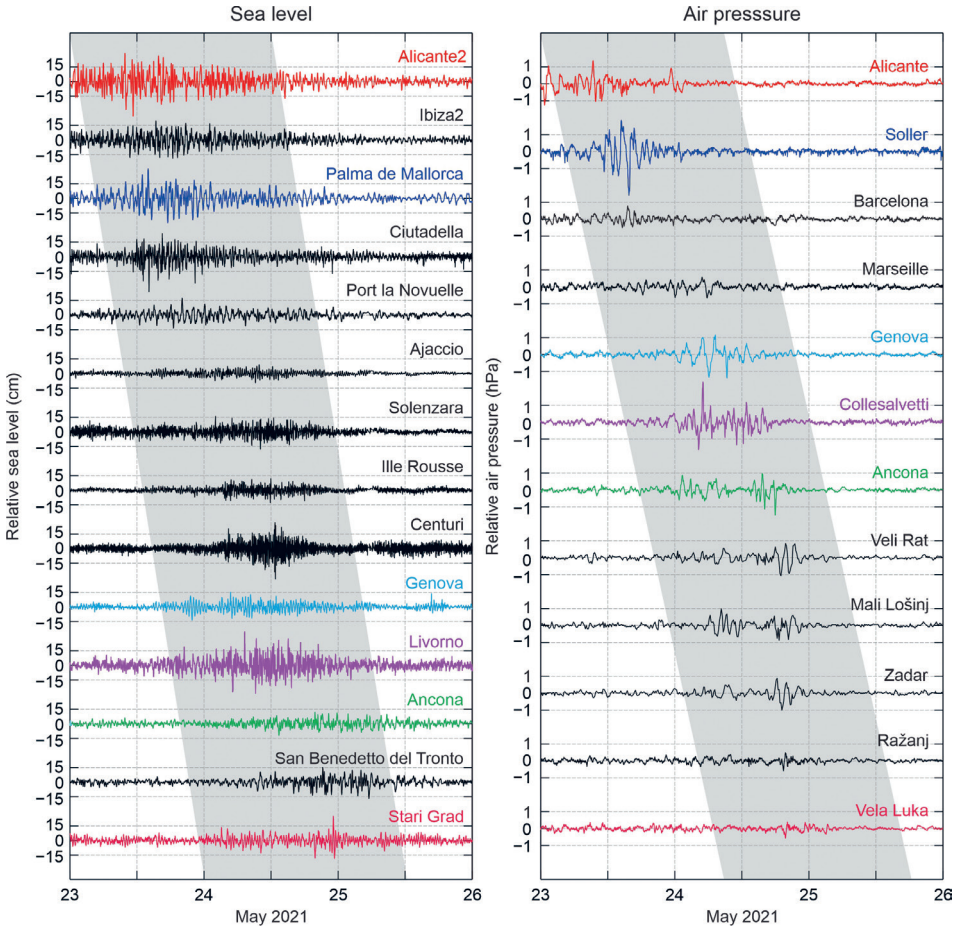

Figure 3. High-pass (2-h Kaiser-Bessel window) component of: (*left*) sea-level and (*right*) air pressure time series, measured from the 23rd to the 26th of May 2021 along the western Mediterranean Sea and the Adriatic Sea. Time series measured at locations where tide gauge and atmospheric pressure stations are within 30 km distance of each other are coloured the same. Shaded areas indicate periods of increased high-frequency activity.

The high-frequency time series of air pressure (Fig. 3) show a similar pattern – strong oscillations (height of 3.7 hPa at Soller) were first recorded at the southwestern stations, then over the French and Italian Mediterranean stations (height of 3.4 hPa at Collesalvetti) and finally over the Adriatic stations (height of 1.4 hPa at Veli Rat and Zadar). The nearest meteorological stations to Bonifacio and Široka Bay are, respectively, Collesalvetti (~260 km distance) and Veli Rat (~10 km distance). The sampling time step at two of the Adriatic Sea meteorological stations is 10 min, so the recorded magnitude of the air pressure variations at these two stations is expected to be attenuated compared to the variations that actually oc-

curred. The timing of the amplified air pressure fluctuations is consistent with the timing of the amplified sea-level oscillations over all areas.

The atmospheric oscillations recorded at different areas are unlikely to represent the same atmospheric pressure disturbances, with the exception of the Adriatic Sea. The disturbances recorded at Ancona, Veli Rat, Mali Lošinj and Zadar (Adriatic Sea) all have similar shapes and the distance between stations (at most 100 km) is such that a mesoscale atmospheric pressure disturbance can bridge it without losing much of its properties (*e.g.*, Vilibić et al., 2004). The abundance of the atmospheric pressure disturbances over the western Mediterranean and Adriatic Seas indicates that the atmosphere was prone to the development and propagation of atmospheric pressure disturbances between the 23rd and the 26th of May 2021.

We used the global ERA5 reanalysis dataset to assess the synoptic conditions associated with the May 2021 event. Figure 4 shows these conditions at times of

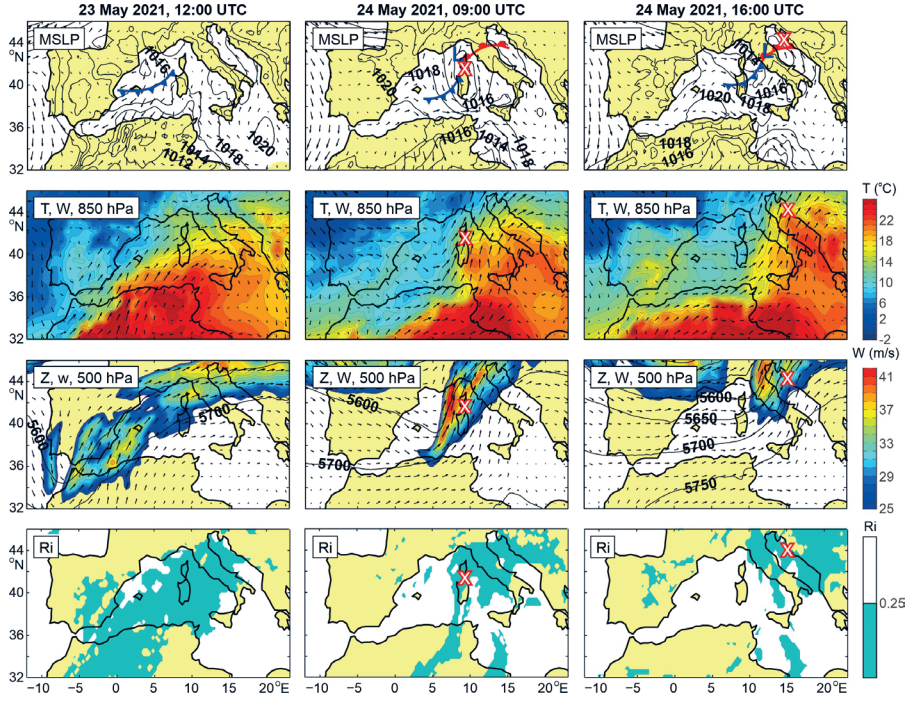

Figure 4. Synoptic conditions during the May 2021 meteotsunami event. (*First row*) mean sea-level pressure and temperature fronts; (*second row)* temperature (shaded) and wind at 850 hPa; *(third row*) geopotential height and wind at 500 hPa (wind speeds above 25 m/s are shown in colour); *(fourth row*) unstable atmospheric layers (coloured areas denote $Ri < 0.25$); (*first column)* 23rd of May 2021, 12:00 UTC; (*second* column) 24th of May 2021, 09:00 UTC; (*third column*) 24th of May 2021, 16:00 UTC. The crosses mark the locations where meteotsunamis occurred and are indicated at the times closest to meteotsunami occurrence.

occurrence of intensified high-frequency sea-level oscillations and meteotsunamis over: the southwestern stations (23rd of May 2021, 12:00 UTC), Corsica and Bonifacio (24th of May 2021, 09:00 UTC) and the Adriatic Sea and Široka Bay (24th of May 2021, 16:00 UTC). The observed conditions were clearly meteotsunamigenic (according to literature references listed in the introduction) and included: (i) a weak surface pressure low; (ii) an inflow of warm and dry air at 850 hPa over the humid Mediterranean air at lower altitudes; (iii) high wind speeds (> 25 m/s) at 500 hPa level, directly over the affected locations; and (iv) dynamically unstable atmospheric layers at 600–400 hPa, characterised by $Ri < 0.25$. The most prominent features of the pattern were high wind speeds (25–45 m/s) at unstable mid-tropospheric layers ($Ri < 0.25$). Figure 5 shows relative humidity at the 700 hPa level and high-rate infrared satellite imagery dur-

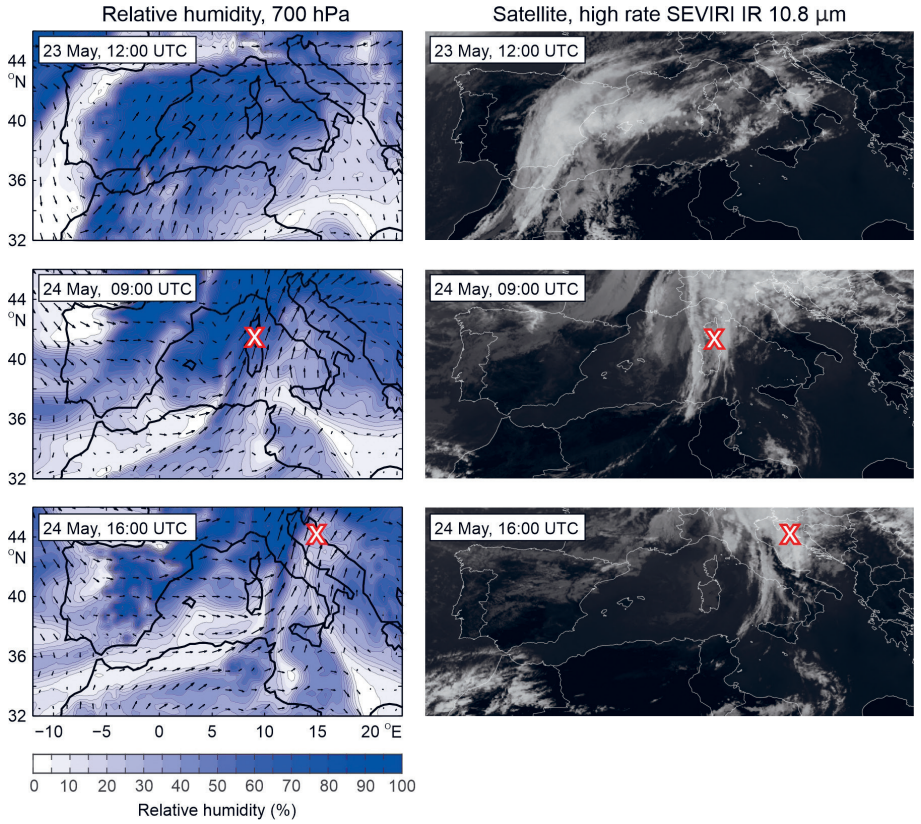

Figure 5. (*first column*) relative humidity at 700 hPa level; (*second column*) high rate SEVIRI infrared satellite imagery over the Mediterranean Sea on: (*first row*) 23rd of May 2021, 12:00 UTC; (*second row*) 24th of May 2021 (09:00 UTC); (*third row*) 24th of May 2021 (16:00 UTC). The crosses mark the locations where meteotsunamis occurred and are indicated at the times closest to meteotsunami occurrence.

ing the event. Both are consistent with synoptic processes at a broader scale and display the presence of a moisture front and a scattered cloud line over the areas affected by meteotsunamis. No convective clouds are visible on the satellite imagery, indicating that the atmosphere was likely not convectively unstable.

Finally, Fig. 6 shows the Froude number, *i.e.*, the ratio between the wind speed at 500 hPa and the speed of long-ocean waves, at the ERA5 times closest to the observed meteotsunamis (*i.e.*, pronounced high-frequency sea-level oscillations for areas where no meteotsunamis were observed). The Froude number

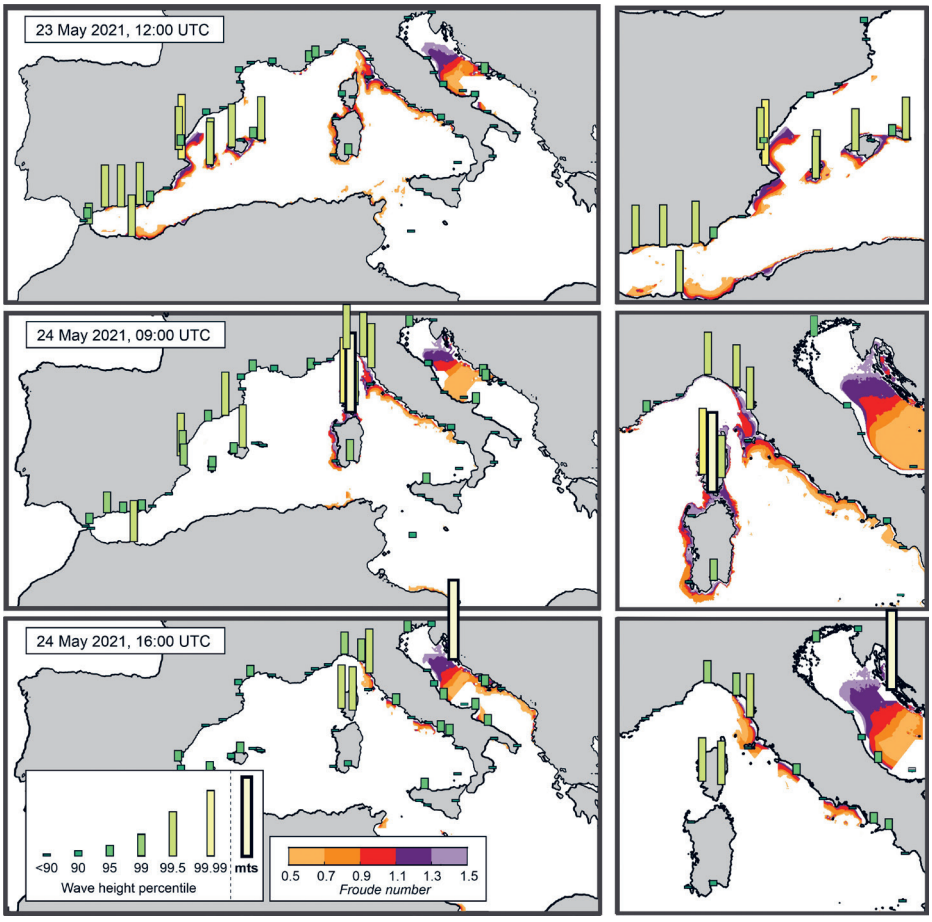

Figure 6. Froude number at the western Mediterranean and the Adriatic Seas on: (*top row*) 23rd of May 2021, 12:00 UTC; (*middle row*) 24th of May 2021, 09:00 UTC; (*bottom row*) 24th of May 2021, 16:00 UTC. The plots on the right are zoom-ins of plots on the left. The maximum wave heights in one hour centred around the given times are shown in relation to the heights of the typical oscillations at each station. The meteotsunami heights are also shown, with an assumption that their heights are near the 100th percentile of the respective background heights.

is depicted only for areas where $0.5 < Fr < 1.5$ and where at least one atmospheric layer between 600 and 400 hPa was unstable ($Ri < 0.25$). The three underlying assumptions are: (1) an atmosphere with strong mid-tropospheric winds embedded in unstable layers supports the formation and propagation of meteotsunamigenic pressure perturbations (*e.g.*, Šepić et al., 2015a); (2) the propagation velocity of such pressure perturbations can be approximated by the wind velocity at the bottom of the unstable layer (Monserrat and Thorpe, 1996); (3) meteotsunamis occur in areas where there is a match between the speed of the air pressure disturbance and the speed of long-ocean waves – given the typical speeds of meteotsunamigenic atmospheric pressure disturbances (10–50 m/s), this is usually the case over shelves up to 200 m deep. Figure 6 also reveals the height of high-frequency sea-level oscillations in comparison to the height of the background sea-level oscillations, *i.e.*, to the "*2-h wave height maxima*" series. It is obvious that meteotsunamis, as well as a general enhancement of high-frequency sea-level activity, occur during the presence of favourable synoptic conditions over the area. After the favourable synoptic system leaves the area, the high-frequency sea-level oscillations weaken within 24 h (as seen in Fig. 6 for the stations in the western Mediterranean).

4. Meteotsunamis of June 2022

In June 2022, two locations in the Mediterranean were hit by meteotsunamis. On the 26th of June, 0.95 m high tsunami-like waves were recorded in Ciutadella (Menorca, 2022; Fig. 7) and on the 28th of June, Bonifacio on the island of Corsica experienced a meteotsunami similar to the 2021 one (height ~1 m; corse matin, 2022). No meteotsunamis were reported in the Adriatic Sea in June 2022. We refer to the Ciutadella event as a meteotsunami despite our threshold of 1 m, as it is likely that oscillations at the very top of the old Ciutadella harbour were higher than 0.95 m. Further on, the height of 0.95 m classifies the event as a "rissaga" (meteotsunami) according to the literature (*e.g.*, Rabinovich and Monserrat, 1996) and the Balearic RIssaga Forecasting System (BRIFS) (https://www.socib.es/index.php?seccion=modelling&facility=rissagaforecast).

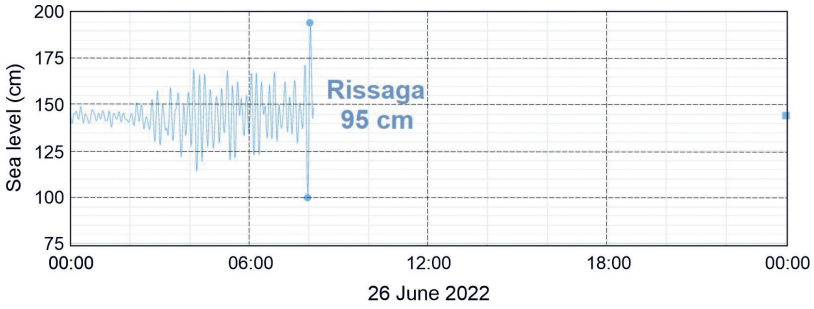

Figure 7. Sea-level time series measured at Ciutadella (Menorca, 2022).

High-frequency (2-h Kaiser-Bessel window) sea-level and air pressure data measured from the 26th to the 27th of June 2022 are shown in Fig. 8. For Ciutadella we show tide gauge data measured at a nearby Son Blanc, outside the old port of Ciutadella (as the Ciutadella data shown in Fig. 7 were not available to us in numerical form). At most stations, sea-level oscillations were weaker than during the 2021 event, with the exception of Ciutadella (Fig. 7) where sea-level oscillations were three times as high. At Solenzara (the station closest to Bonifacio), Livorno (another station close to Bonifacio) and San Benedetto del Tronto sea-level oscillations were about the same height as during the May 2021 event.

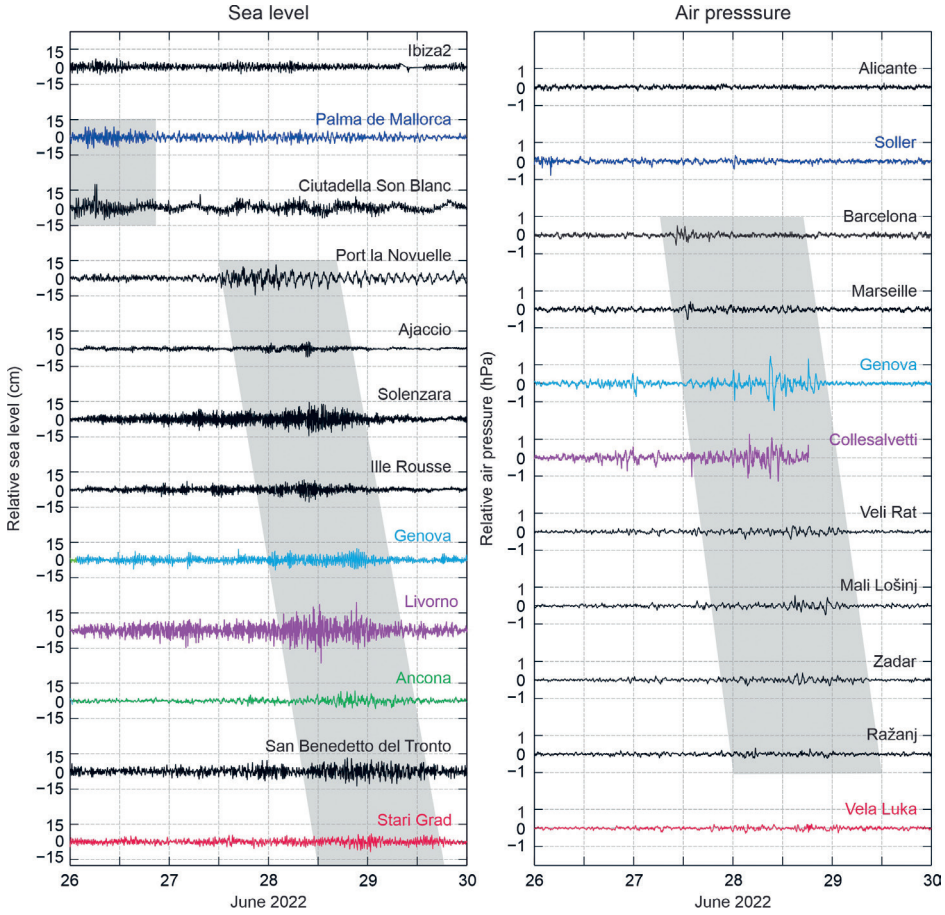

Figure 8. High-pass (2-h Kaiser-Bessel window) component of: (*left*) sea-level and (*right*) air pressure time series, measured from the 26th to the 27th of June 2022 in the western Mediterranean Sea and the Adriatic Sea. Time series measured at locations where tide gauge and atmospheric pressure stations are within 30 km distance of each other are coloured the same. Shaded areas indicate periods of increased high-frequency activity.

Moreover, the oscillations recorded in Stari Grad (Adriatic Sea) in 2022 were stronger than those recorded in 2021 – but still very weak compared to the oscillations normally observed during a therein meteotsunami (Šepić and Orlić, 2023). The intensification of high-frequency sea-level activity again had a general northeasterly propagation pattern, with the high-frequency air pressure oscillations coinciding with the sea-level oscillations. Similar to the sea-level, air pressure oscillations were weaker during the event of June 2022 than during the event of May 2021 at most stations, with the exception of two stations closest to the port of Bonifacio: Genoa (height of 2.8 hPa) and Collesalveti (height of 2.2 hPa). Over the Adriatic Sea, air pressure oscillations of no more than 1 hPa height were recorded. But again, for some of the Adriatic stations, the attenuation of the recorded signal compared to the real signal, due to the relatively coarse sampling interval of 10-min, should be taken into account.

The results of the synoptic analyses are presented in Fig. 9. We can identify characteristic meteotsunamigenic synoptic patterns precisely over the areas

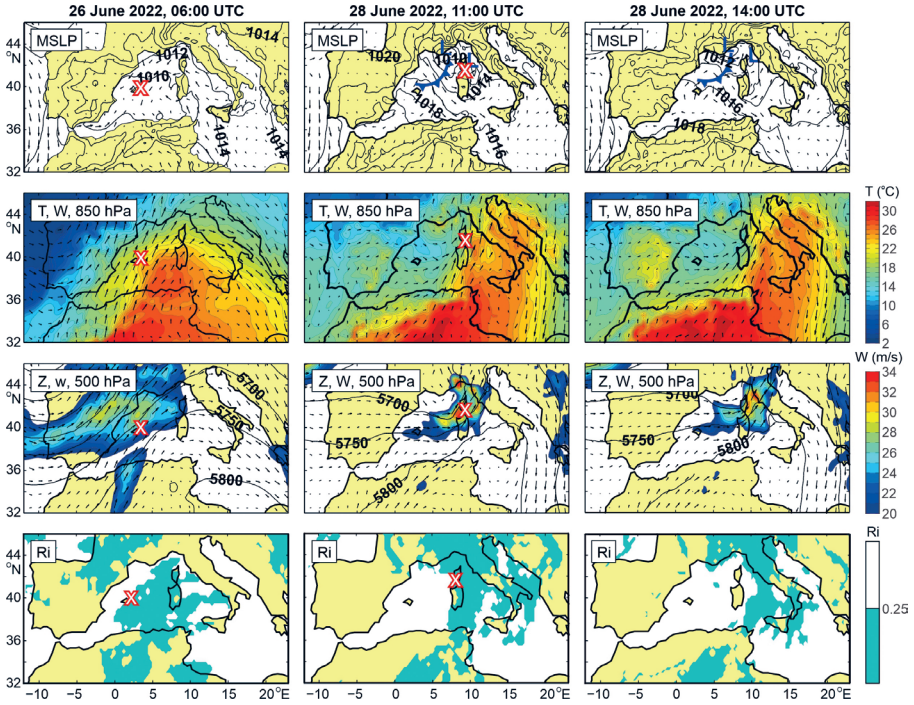

Figure 9. Synoptic conditions during the June 2022 meteotsunami events: (*first row*) mean sea-level pressure and temperature fronts; (*second row)* temperature (shaded) and wind at 850 hPa; *(third row*) wind velocity at 500 hPa (wind speeds above 20 m/s are shown in colour); *(fourth row*) unstable atmospheric layers (coloured areas denote $Ri < 0.25$); (*first column)* 26th of June 2022, 12:00 UTC; (*second* column) 28th of June 2022, 11:00 UTC; (*third column*) 28th of June 2022, 14:00 UTC. The crosses mark the locations where meteotsunamis occurred and are indicated at the times closest to meteotsunami occurrence.

where intensification of high-frequency atmospheric and sea-level activity occurred: during the morning hours of the 26th of June 2022 over the Spanish Mediterranean coast (26th of June 2022; 08:00 UTC); during the midday hours of the 28th of June 2022 over Corsica and the French Mediterranean coast (28th of June 2022; 11:00 UTC); and during the evening hours of the same day over the northern Adriatic Sea (28th of June 2022; 14:00 UTC). Relative humidity at the 700 hPa level and cloud cover indicate convective activity in the atmosphere, with convective clouds identifiable by orange and yellow colours in the convective RGB composite (Fig. 10).

Comparing the synoptic situations of the May 2021 and the June 2022 events, we notice general similarities between the conditions, but also three relevant differences: (1) the 500-hPa jet stream was much stronger during the 2021 event, especially over the Adriatic Sea; (2) the atmosphere was convec-

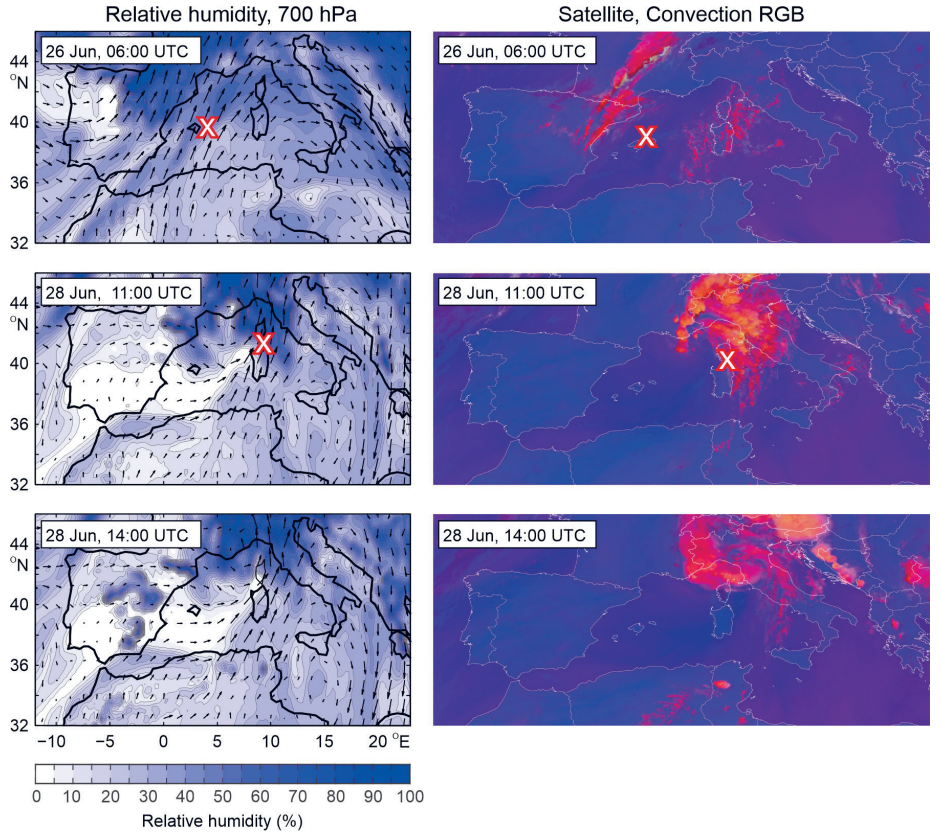

Figure 10. (*first column*) relative humidity at 700 hPa level; (*second column*) convection RGB satellite imagery over the Mediterranean at: (*first row*) 26th of June 2022, 06:00 UTC; (*second row*) 28th of June 2022 (11:00 UTC); (*third row*) 28th of June 2022 (14:00 UTC). Crosses mark locations at which meteotsunamis occurred and are indicated at times closest to their occurrence.

tively unstable during the June 2022 event, but likely not during the May 2021 event; (3) the propagation of the meteotsunamigenic pattern from the western Mediterranean Sea to the northern Adriatic Sea lasted shorter in May 2021 (~1.5 days) than in June 2022 (~2.5 days).

Froude number, computed for the June 2022 event, for areas for which $Ri < 0.25$, again reveals that the high-frequency sea-level oscillations intensify during the presence of a meteotsunamigenic synoptic system over the area and weaken significantly once the system leaves the area (Fig. 11). In contrast to the May

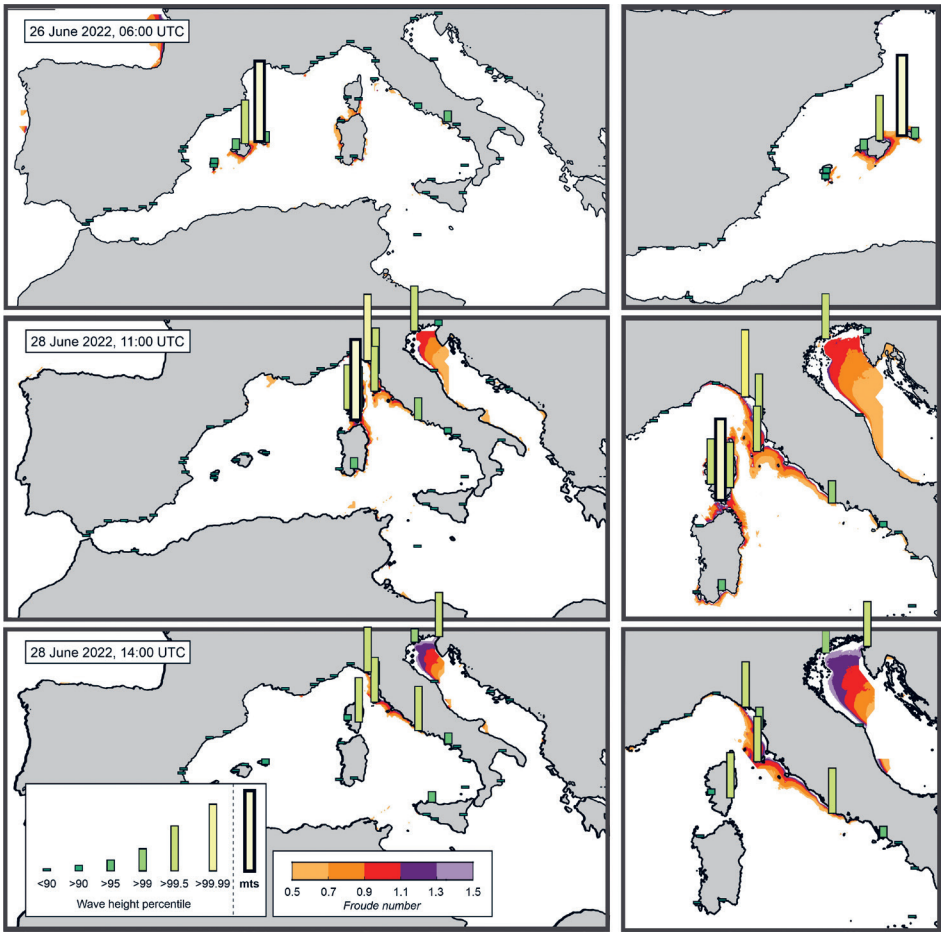

Figure 11. Froude number at the western Mediterranean at: (*top row*) 26th of June 2022, 06:00 UTC; (*middle row*) 28th of June 2022, 11:00 UTC; (*bottom row*) 28th of June 2022, 14:00 UTC. Figures on the right are zoom-ins. The maximum wave heights centred in one hour around the given times are shown in relation to the heights of the typical oscillations at each station. The meteotsunami heights are also shown, with an assumption that their heights are near the 100th percentile of the respective background heights.

2021 event, synoptic conditions during the June 2022 event were meteotsunami favourable over the very northern Adriatic, but not ~100 km to the southeast over Široka Bay. This is also confirmed by the fact that high-frequency sea-level oscillations at two tide gauge stations in the northern Adriatic (Venice and Trieste) intensified during the June 2022 event (but not during the May 2021 events).

5. Discussion

In May 2021 and June 2022, several bays in the western Mediterranean and Adriatic were hit by destructive meteotsunamis: In the morning hours of the 24th of May 2021, a meteotsunami hit Bonifacio on the island of Corsica (western Mediterranean) and in the afternoon hours of the same day, another meteotsunami hit Široka Bay (Ist Island, Adriatic Sea), 500 km away. A year later, on the 26th of June 2022, a meteotsunami hit Ciutadella on the island of Menorca (western Mediterranean) and two days later, on the 28th of June 2022, a meteotsunami occurred in Bonifacio (Corsica Island), 400 km away. No meteotsunamis were recorded in the Adriatic Sea in June 2022. Ciutadella and Široka Bay are known meteotsunami sites (Jansà and Ramis, 2021; Šepić and Orlić, 2023), while Bonifacio is unknown in the international research community as a meteotsunami-prone site. However, as mentioned in the introduction, an Internet search revealed that meteotsunami-like events are not uncommon at Bonifacio.

Figure 12 shows the 99th percentile and maximum wave heights of the "*2-h wave height maxima*" for stations in the western Mediterranean and Adriatic

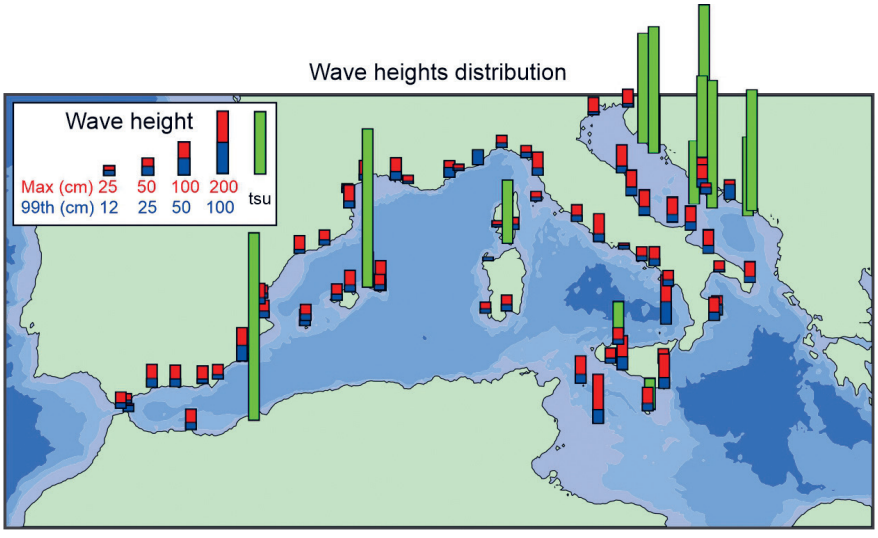

Figure 12. Maximum measured wave height (red bars) and the 99th percentile of the "*2-h wave height maxima*" (blue bars); all for high-frequency sea-level oscillations. Maximum meteotsunami wave heights (only for heights > 1 m), as reported in this paper and in the literature, are also indicated (green bars).

Seas. The known maximum wave heights of the Ciutadella (~5 m; 15th of June 2006; Jansà et al., 2007; Vilibić et al., 2008), Bonifacio (~1 m; events studied here) and Široka Bay (~4 m; 5th of October 1984; Šepić and Orlić, 2023) meteotsunamis, as well as the maximum wave heights of other known meteotsunamis in the western Mediterranean and Adriatic (as reported by Vilibić et al., 2016; and Šepić and Orlić, 2023) are also shown. At most stations, the ratio between the maximum recorded wave height and the 99th percentile wave height is above 2, indicating that there is a high potential for strong amplification of sea-level oscillations. Nevertheless, strong meteotsunamis (wave height > 1 m) occur only at the selected sites, placed mostly along the northern and northeastern coasts, along stretches of the coastline in front of which shelves (< 200 m depth) are located, in bays and harbours with a high quality factor ("*Q factor*"), which is a measure of energy dumping in the system (Rabinovich, 2009). An exception is Mostaganem in northern Algeria (*i.e.*, on the southern coast of the Mediterranean), where a deadly meteotsunami may have occurred along the open coast in 2007 (Okal, 2021).

Wide shelves less than 200 m deep, such as those found in the Mediterranean and Adriatic Seas, support Proudman resonance between long-ocean waves and atmospheric pressure perturbances propagating at speeds less than 44 m/s. To determine the potential for the Proudman resonance of Ciutadella, Bonifacio and Široka Bay, we estimated the Proudman length at points near the entrances to the bays (Fig. 13a). Resonance conditions are best satisfied for atmospheric disturbances propagating: (a) from south-southwest to west at speeds of 20–40 m/s toward Ciutadella; (b) from southwest to west-southwest at speeds of 20 m/s (also possible for 10 to 50 m/s) toward Bonifacio; and (c) from south-southeast to west at speeds of 20–40 m/s toward Široka Bay. Looking only at Fig. 13a, Široka Bay seems to be the place where the strongest meteotsunamis can occur and Bonifacio the place where the weakest ones are to be expected.

The question arises whether atmospheric pressure disturbances actually propagate at meteotsunamigenic velocities over these areas. The velocities of atmospheric pressure disturbances are usually estimated after the event using available measurements. At least three stations, less than ~50 km apart, are needed for the estimation. For the May 2021 and June 2022 events, such atmospheric stations were not available to us. However, it has been shown previously that meteotsunamigenic atmospheric pressure disturbances propagate with the velocities of the mid-tropospheric winds (Monserrat and Thorpe, 1996). For this reason, we decided to use the wind velocity at 500 hPa as a proxy for the propagation velocity of atmospheric pressure disturbances. Our assumption is supported by the analyses presented in Figs. 6 and 11. Intense high-frequency sea-level oscillations occur exactly where $0.7 < Fr < 1.3$, *i.e.*, where the wind speed at 500 hPa is within 70–130% of the long-ocean wave speed. This is the same range of speeds that atmospheric pressure disturbances should have for Proudman resonance to occur (Vilibić, 2008). Given that the long-ocean waves were

indeed significantly intensified, and that meteotsunamis occurred, it is reasonable to assume that air pressure disturbances propagated at this range of speeds as well. We have marked the 500-hPa wind speed and direction (from the ERA5 data) at the times of the events studied here and at the times of the other known events (observed during 1993–2022) in all plots of Fig. 13 (a list of events, speeds, directions and sources/references, is given in the Appendix). It is obvious that meteotsunamis occur when atmospheric disturbances propagate toward the

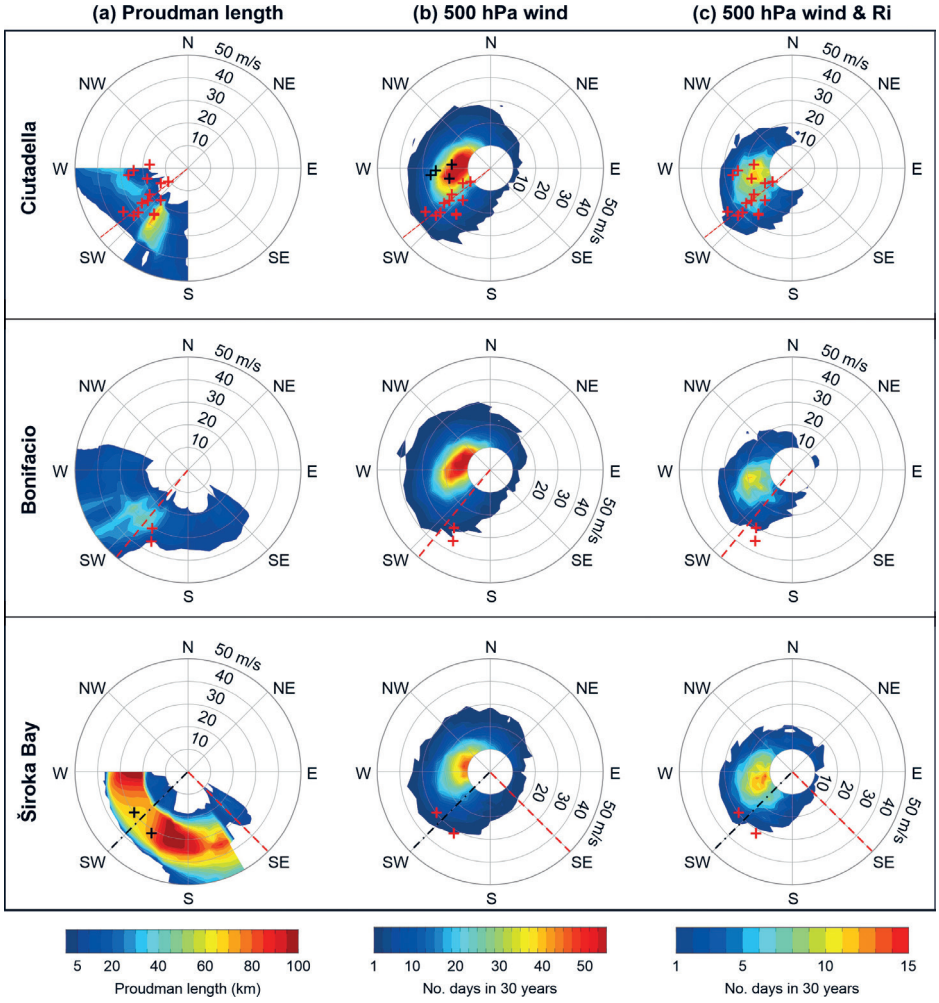

Figure 13. (*a*) Proudman length; (*b*) climatology of the 500-hPa wind; and (*c*) climatology of the 500-hPa wind on days when atmospheric layers between 600 and 400 hPa are unstable; for (*first row*) Ciutadella; (*second row*) Bonifacio and (*third row*) Široka Bay. Red dashed lines denote orientation of bay mouths; and black dot-dashed line orientation of the narrow strait between the islands of Ist and Molat (as indicated in Fig. 1).

mouth of the bay at velocities for which Proudman resonance is supported. For Široka Bay, the preferred direction of propagation is, however, not toward the mouth of the bay, but toward the narrow strait between Ist Island and nearby Molat Island, indicating a likely reflection of long-ocean waves from Molat Island toward Široka Bay (as previously suggested by Šepić et al., 2009b).

We next have a look at typical May to November synoptic conditions over the Mediterranean. Figure 13b shows the number of days (in 30 years; 1993–2022) with a given 500-hPa wind and direction over the three locations studied (*i.e.*, the ERA5 points closest to Ciutadella, Bonifacio and Široka Bay) and Figure 13c shows the number of days with a given 500-hPa wind direction and speed, but with the additional condition that at least one of the atmospheric layers between the 600 and 400 hPa levels was unstable ($Ri < 0.25$). Thus, the 30-year climatology of mid-tropospheric velocities is given in Figure13b and the 30-year climatology of mid-tropospheric velocities in situations where these atmospheric layers are also unstable, *i.e.*, when the generation and propagation of atmospheric pressure disturbances are supported, is given in Fig. 13c. The two distributions are similar, but there are also significant differences. The mid-tropospheric winds over the western Mediterranean and Adriatic most frequently have speeds of 10–20 m/s and generally have a northwesterly to southwesterly direction, with the slower winds tending to be northwesterly and the faster winds southwesterly (Fig. 13b). On days when the mid-tropospheric atmospheric layers are unstable, winds from the west-southwest with ~20 m/s speeds are strongly favoured (reddish bulbs in Fig. 13c for all stations).

At Ciutadella, there is a high match between the preferred velocities of the atmospheric disturbances (*i.e.*, the 500-hPa wind velocity), the shelf width and orientation (*i.e.*, the Proudman length) and the orientation of the mouth of the bay. This, together with the high amplification factor of the bay itself (Rabinovich et al., 1999), may explain why Ciutadella meteotsunamis are both frequent and strong (Jansà and Ramis, 2021). As for Široka Bay, an extremely wide shelf with slowly changing depths, that allows for Proudman resonance and significant amplification of long-ocean waves, can be found in front of it. However, the preferred direction and speed of the 500-hPa wind on days with unstable layers in the mid troposphere is such that it does not support the propagation of meteotsunamigenic disturbances toward the mouth of the bay (zero days in 30 years) and only rarely (<5 days in 30 years) supports their propagation toward the coast of Molat Island. Assuming that forced long-ocean waves propagate in the direction of atmospheric pressure disturbances we can conclude that these waves do not propagate directly toward Široka Bay and that they rarely propagate toward Molat (from which they can be reflected into Široka Bay). Thus, it can be assumed that Ist meteotsunamis occur rarely, but, when they do occur, they are extremely strong. This is consistent with known list of Ist meteotsunamis (Šepić and Orlić, 2023). While the shelf potential for Proudman resonance is not as strong in Bonifacio as in Široka Bay, it is comparable to that of Ciutadella. The orientation

of the mouth of Bonifacio Bay is almost aligned with the direction of the largest Proudman length. Nevertheless, similar to the case of Ist, there is a low match between the meteotsunamigenic 500-hPa wind velocities and the direction of the largest Proudman length. Given the above, it is likely that Bonifacio meteotsunamis are less frequent than those of Ciutadella and weaker than those of both Ciutadella and Široka Bay. The absence of Bonifacio events in the scientific literature could confirm this hypothesis. However, an on-site survey should be carried out, including interviews with the local population, to evaluate the historical distribution of meteotsunamis in Bonifacio.

The analyses carried out can be repeated for other places of interest or even for entire stretches of coastline. However, it should be kept in mind that our analyses were performed assuming that: (1) the velocity of wind at 500 hPa can be used as a proxy for the velocity of atmospheric pressure disturbances; (2) the frequency of formation of meteotsunamigenic pressure disturbances is proportional to the presence of meteotsunamigenic synoptic conditions over the area and (3) without taking into account additional factors such as orography that may influence the generation of atmospheric gravity waves and convective jumps (Belušić et al., 2007).

6. Conclusion

We summarize our findings as follows:

(1) Mediterranean meteotsunamis and intensification of high-frequency sea-level oscillations occur when meteotsunamigenic synoptic conditions prevail over the area (Figs. 4 and 9).

(2) The most important synoptic condition is the presence of a southwesterly jet stream at mid troposphere, embedded in unstable atmospheric layers (Figs. 6 and 11). These layers might be dynamically (likely for the May 2021 event) or convectively unstable (more likely for the June 2022 event) (Figs. 5 and 10).

(3) The strongest meteotsunamis tend to occur along the northern and northeastern coasts of the Mediterranean Sea, along stretches of the coastline in front of which shelves (< 200 m depth) are located (Fig. 12).

(4) These shelves allow a Proudman resonance between long-ocean waves and atmospheric disturbances coming from the east-south-west at speeds of 20 to 40 m/s (Fig. 13a).

(5) General synoptic conditions over the western Mediterranean during the warmer half of the year (May–October) favour the propagation of meteotsunamigenic synoptic disturbances from the southwest-northwest with speeds of 10–30 m/s; with disturbances coming from the west-southwest being the most favoured (Figs. 13b and 13c).

(6) The strongest and most frequent meteotsunamis occur at locations where shelf and coastal orientation (high Proudman length; Fig. 13a), bay mouth orientation (Fig. 13a), favourable synoptic conditions (Figs. 13b and 13c) and bay shape coincide.

Acknowledgements – We thank Yann Balouin and Hamon Kerivel Klervi, both from BRGM – The French Geological Survey, for drawing our attention to the Bonifacio meteotsunami events, as well as Luka Kovačić, Antea Copić, Jure Jakić, Pave Pilić, Roko Topić and Jure Vranić, all students of the Faculty of Science – University of Split at the time of initial analysis, for their contribution to the discussion and helpful insights in the early stages of our research. We sincerely thank three anonymous reviewers for their constructive comments that helped us significantly improve quality of the research. The research was supported by the ERC STG-853045 SHExtreme project and the Croatian Science Foundation HRZZ-IP-2019-04-5875 StVar-Adri project.

References

Belušić, D., Grisogono, B. and Bencetić Klaić, Z. (2007): Atmospheric origin of the devastating coupled air-sea event in the east Adriatic, *J. Geophys. Res.*, **112**, D17111, https://doi.org/10.1029/2006JD008204.

Candela, J., Mazzola, S., Sammari, C., Limeburner, R., Lozano, C. J., Patti, B. and Bonanno, A. (1999): The "Mad Sea" phenomenon in the Strait of Sicily, *J. Phys. Oceanogr.*, **29**, 2210–2231, https://doi.org/10.1175/1520-0485(1999)029<2210:TMSPIT>2.0.CO;2.

Centro Meteo Italiano (2021): A mini meteotsunami hits Bonifacio in Southern Corsica, https://www.centrometeoitaliano.it/notizie-meteo/meteo-raro-fenomeno-di-meteotsunami-travolge-bonifacio-corsica-video-di-quanto-accaduto-106686/?refresh_cens, last accessed on 20 August 2022 (in Italian).

Copernicus Climate Change Service (C3S) (2017): ERA5: Fifth generation of ECMWF atmospheric reanalyses of the global climate. Copernicus Climate Change Service Climate Data Store (CDS), https://cds.climate.copernicus.eu/cdsapp#!/home, last accessed on 20 August 2022.

corse matin (2021): Bonifacio: Floods caused by a marine seiche, https://www.corsematin.com/articles/bonifacio-les-inondations-causees-par-une-seiche-marine-117897, last accessed on 20 August 2022 (in French).

corse matin (2022): Floods following a rise in water at the port of Bonifacio, https://www.corsematin.com/articles/video-inondations-a-la-suite-dune-montee-des-eaux-au-port-de-bonifacio-126883, last accessed on 15 September 2022 (in French).

Dnevnik.hr (2021): Tidal wave hits island of Ist, https://dnevnik.hr/vijesti/hrvatska/plimni-val-pogodio-otok-ist-mjestani-su-na-vrijeme-vidjeli-da-se-more-povlaci-pa-su-pripremili-daske-i-pumpe---653220.html, last accessed on 05 December 2022 (in Croatian).

Drago, A. (1999): A study on the sea level variations and the "Milghuba" phenomenon in the coastal waters of the Maltese Islands. Doctoral dissertation, University of Southampton, https://www.um.edu.mt/library/oar/handle/123456789/92754.

Durran, D. R. and Klemp, J. B. (1982): On the effects of moisture on the Brunt-Väisälä frequency, *J. Atmos. Sci.,* **39**, 10, 2152–2158, https://doi.org/10.1175/1520-0469(1982)039<2152:OTEOMO>2.0.CO;2.

Greenspan, H. P. (1956): The generation of edge waves by moving pressure disturbances, *J. Fluid Mech.*, **1**, 574–592, https://doi.org/10.1017/S002211205600038X.

Hersbach, H., Bell, B., Berrisford, P., Hirahara, S., Horányi, A., Muñoz-Sabater, J., Nicolas, J., Peubey, C., Radu, R., Schepers, D., Simmons, A., Soci, C., Abdalla, S., Abellan, X., Balsamo, G., Bechtold, P., Biavati, G., Bidlot, J., Bonavita, M., De Chiara, G., Dahlgren, P., Dee, D., Diamantakis, M., Dragani, R., Flemming, J., Forbes, R., Fuentes, M., Geer, A., Haimberger, L., Healy, S., Hogan, R. J., Hólm, E., Janisková, M., Keeley, S., Laloyaux, P., Lopez, P., Lupu, C., Radnoti, G., de Rosnay,

P., Rozum, I., Vamborg, F., Villaume, S. and Thépaut, J.-N. (2020): The ERA5 global reanalysis, *Q. J. Roy. Meteor. Soc.*, **146**, 1999–2049, https://doi.org/10.1002/qj.3803.

Hibiya, T. and Kajiura, K. (1982): Origin of 'Abiki' phenomenon (a kind of seiche) in Nagasaki Bay, *J. Oceanogr. Soc. Japan*, **38**, 172–182, https://doi.org/10.1007/BF02110288.

Hodžić, M. (1979/1980): Occurrences of exceptional sea level oscillations in the Vela Luka Bay, *Priroda*, **68**(2–3), 52–53 (in Croatian).

Jansà, A. and Ramis, C. (2021): The Balearic rissaga: From pioneering research to present-day knowledge, *Nat. Hazards*, **106**, 1269–1297, https://doi.org/10.1007/s11069-020-04221-3.

Jansà, A, Monserrat, S. and Gomis, D. (2007): The rissaga of 15 June 2006 in Ciutadella (Menorca), a meteorological tsunami, *Adv. Geosci.,* **12**, 1–4, https://doi.org/10.5194/adgeo-12-1-2007.

Lamb, H. (1932): *Hydrodynamics*. Cambridge University Press, Cambridge, 738 pp.

Linares, Á., Wu, C. H., Bechle, A. J., Anderson, E. J. and Kristovich, D. A. (2019): Unexpected rip currents induced by a meteotsunami, *Sci. Rep.*, **9**, 2105, https://doi.org/10.1038/s41598-019-38716-2.

Menorca (2022): 'Rissaga' in Ciutadella of 95 cm, the highest this year, https://www.menorca.info/menorca/local/2022/06/26/1750819/rissaga-ciutadella-mas-alta-este-ano.html, last accessed on 20 August 2022 (in Spanish).

Monserrat, S. and Thorpe, A. J. (1996): Use of ducting theory in an observed case of gravity waves, *J. Atmos. Sci.*, **53**, 1724–1736, https://doi.org/10.1175/1520-0469(1996)053<1724:UODTIA>2.0.CO;2.

Monserrat, S., Rabinovich, A. B. and Casas, B. (1998): On the reconstruction of the transfer function for atmospherically generated seiches, *Geophys. Res. Lett.*, **25**, 2197–2200, https://doi.org/10.1029/98GL01506.

Monserrat, S., Vilibić, I. and Rabinovich, A. B. (2006): Meteotsunamis: atmospherically induced destructive ocean waves in the tsunami frequency band, *Nat. Hazards Earth Syst. Sci.*, **6**, 1035–1051, https://doi.org/10.5194/nhess-6-1035-2006.

Okal, E. A. (2021): On the possibility of seismic recording of meteotsunamis, *Nat. Hazards*, **106**, 1125–1147. https://doi.org/10.1007/s11069-020-04146-x.

Orlić, M. (1980): About a possible occurrence of the Proudman resonance in the Adriatic, *Thalassia Jugoslavica*, **16**, 1, 79–88.

Orlić, M. (2015): The first attempt at cataloguing tsunami-like waves of meteorological origin on Croatian coastal waters, *Acta Adriat.*, **56**, 83–96.

Orlić, M., Belušić, D., Janeković, I. and Pasarić, M. (2010): Fresh evidence relating the great Adriatic surge of 21 June 1978 to mesoscale atmospheric forcing, *J. Geophys. Res.*, **115**, C0601, https://doi.org/10.1029/2009JC005777.

Pattiaratchi, C. B. and Wijeratne, E. M. S. (2015): Are meteotsunamis an underrated hazard?, *Philos. T. Roy. Soc. A*, **373**, https://doi.org/10.1098/rsta.2014.0377.

Pellikka, H., Šepić, J., Lehtonen, I. and Vilibić I. (2022): Meteotsunamis in the northern Baltic Sea and their relation to synoptic patterns, *Weather Clim. Extrem.*, **38**, 100527, https://doi.org/10.1016/j.wace.2022.100527.

Proudman, J. (1929): The effects on the sea of changes in atmospheric pressure, *Geophys. Supp. Mon. Notices Royal Astron. Soc.*, **2**, 197–209, https://doi.org/10.1111/j.1365-246X.1929.tb05408.x.

Rabinovich, A. B. (2009): Seiches and harbour oscillations, in: *Handbook of coastal and ocean engineering*, edited by Kim, Y. C. World Scientific Publishing, Singapore, pp 193–236.

Rabinovich, A. B. (2020): Twenty-seven years of progress in the science of meteorological tsunamis following the 1992 Daytona Beach event, *Pure Appl. Geophys.*, **177**, 1193–1230, https://doi.org/10.1007/s00024-019-02349-3.

Rabinovich, A. B. and Monserrat, S. (1996): Meteorological tsunamis near the Balearic and Kuril Islands: Descriptive and statistical analysis, *Nat. Hazards*, **13**, 55–90, https://doi.org/10.1007/BF00156506.

Rabinovich, A. B., Monserrat, S. and Fine, I. V. (1999): Numerical modelling of extreme seiche oscillations in the region of the Balearic Islands, *Oceanology*, **39**, 12–19.

Raichlen, F. (1966): Harbor resonance, in: *Estuary and coastline hydrodynamics*, edited by Ippen, A. T. McGraw Hill Book Comp., New York, pp 281–340.

Ramis, C. and Jansà, A. (1983): Condiciones meteorológicas simultáneas a la aparición de oscilaciones del nivel del mar de amplitud extraordinaria en el Mediterráneo occidental, *Revista de Geofísica*, **39**, 35–42 (in Spanish).

Sallanger Jr., A. H., List, J. H., Gelfenbaum, G., Stumpf, R. P. and Hansen, M. (1995): Large wave at Daytona Beach, Florida, explained as a squall-line surge, *J. Coast. Res.*, **11**, 1383–1388. https://www.jstor.org/stable/4298439.

Šepić, J. and Rabinovich, A. B. (2014): Meteotsunami in the Great Lakes and on the Atlantic coast of the United States generated by the "derecho" of June 29–30, 2012, *Nat. Hazards*, **74**, 75–107, https://doi.org/10.1007/s11069-014-1310-5.

Šepić, J. and Orlić, M. (2023): Meteorological tsunamis in the Adriatic Sea, https://projekti.pmfst.unist.hr/floods/meteotsunamis/, last accessed on 11 September 2023.

Šepić, J., Vilibić, I. and Monserrat, S. (2009a): Teleconnections between the Adriatic and the Balearic meteotsunamis, *Phys. Chem. Earth*, **34**, 928–937, https://doi.org/10.1016/j.pce.2009.08.007.

Šepić, J., Vilibić, I. and Belušić, D. (2009b): Source of the 2007 Ist meteotsunami (Adriatic Sea), *J. Geophys. Res.-Oceans*, **114**, https://doi.org/10.1029/2008JC005092.

Šepić, J., Vilibić, I., Rabinovich, A. B. and Monserrat, S. (2015a): Widespread tsunami-like waves of 23–27 June in the Mediterranean and Black Seas generated by high-altitude atmospheric forcing, *Sci. Rep.*, **5**, 11682, https://doi.org/10.1038/srep11682.

Šepić J., Vilibić, I., Lafon, A., Machebouef, L. and Ivanović, Z. (2015b): High-frequency sea level oscillations in the Mediterranean and their connection to synoptic patterns, *Progr. Oceanogr.*, **137**, 284–298, https://doi.org/10.1016/j.pocean.2015.07.005.

Šepić, J., Međugorac, I., Janeković, I., Dunić, N. and Vilibić, I. (2016): Multi-meteotsunami event in the Adriatic Sea generated by atmospheric disturbances of 25–26 June 2014, *Pure Appl. Geophys.*, **173**, 4117–4138, https://doi.org/10.1007/s00024-016-1249-4.

Šepić, J., Rabinovich, A. B. and Sytov, V. N. (2018a): Odessa tsunami of 27 June 2014: Observations and numerical modelling, *Pure Appl. Geophys.*, **175**, 1545–1572, https://doi.org/10.1007/s00024-017-1729-1.

Šepić, J., Vilibić, I., Rabinovich, A. B. and Tinti, S. (2018b): Meteotsunami ("Marrobbio") of 25–26 June 2014 on the southwestern coast of Sicility, Italy, *Pure Appl. Geophys.*, **175**, 1573–1593, https://doi.org/10.1007/s00024-018-1827-8.

Thomson, R. E. and Emery, W. J. (2014): *Data analysis methods in physical oceanography*. Elsevier, Amsterdam, 728 pp.

Vilibić, I. (2008): Numerical simulations of the Proudman resonance, *Cont. Shelf Res.*, **28**, 574–581, https://doi.org/10.1016/j.csr.2007.11.005.

Vilibić, I. and Šepić, J. (2009): Destructive meteotsunamis along the eastern Adriatic coast: Overview, *Phys. Chem. Earth*, **34**, 904–917, https://doi.org/10.1016/j.pce.2009.08.004.

Vilibić, I., Domijan, N., Orlić, M., Leder, N. and Pasarić, M. (2004): Resonant coupling of traveling air pressure disturbance with the east Adriatic coastal waters, *J. Geophys. Res.*, **109**, C10, https://doi.org/10.1029/2004JC002279.

Vilibić, I., Monserrat, S., Rabinovich, A. B. and Mihanović, H. (2008): Numerical modelling of the destructive meteotsunami of 15 June, 2006 on the coast of the Balearic islands, *Pure Appl. Geophys.*, **165**, 2169–2195, https://doi.org/10.1007/s00024-008-0426-5.

Vilibić, I., Šepić, J., Rabinovich, A. B. and Monserrat, S. (2016): Modern approaches in meteotsunami research and early warning, *Frontiers Marine Sci.*, **3**, https://doi.org/10.3389/fmars.2016.00057.

Vilibić, I., Rabinovich, A. B. and Anderson, E. J. (2021): Special issue on the global perspective on meteotsunami science: Editorial, *Nat. Hazards*, **106**, 1087–104, https://doi.org/10.1007/s11069-021-04679-9.

Vučetić, T., Vilibić, I., Tinti, S. and Maramai, A. (2009): The Great Adriatic flood of 21 June 1978 revisited: An overview of the reports, *Phys. Chem. Earth,* **34***,* 894–903, https://doi.org/10.1016/j.pce.2009.08.005.

Weatherall, P., Marks, K. M., Jakobsson, M., Schmitt, T., Tani, S., Arndt, J. E., Rovere, M., Chayes, D., Ferrini, V. and Wigley, R. (2015): A new digital bathymetric model of the world's oceans, *Earth Space Sci.*, **2**, 331–345, https://doi.org/10.1002/2015EA000107.

Zemunik, P., Bonanno, A., Mazzola, S., Giacalone, G., Fontanta, I., Genovese, S., Basilone, G., Candela, J., Šepić, J., Vilibić, I. and Aronica, S. (2020): Observing meteotsunamis ("Marrobbio") on the southwestern coast of Sicily, *Nat. Hazards*, **106**, 1337–1363, https://doi.org/10.1007/s11069-020-04303-2.

Zemunik, P., Denamiel, C., Šepić, J. and Vilibić, I. (2022): High-frequency sea-level analysis: Global distributions, *Global Planet. Change*, **210**, 103775, https://doi.org/10.1016/j.gloplacha.2022.103775.

SAŽETAK

Mediteranski meteotsunamiji iz svibnja 2021. i lipnja 2022. godine: Opažanja, analiza podataka i sinoptička pozadina

Mia Pupić Vurilj, Tina Brnas, Krešimir Ruić, Jadranka Šepić i Marijana Balić

U Sredozemnom moru redovito se opažaju meteotsunamiji, tj. tsunamiji meteorološkog podrijetla. Tijekom pojedinačnih događaja, destruktivni valovi koji izazivaju poplavljivanje obično se javljaju na samo jednoj lokaciji ili ograničenom području. Međutim, u svibnju 2021. i lipnju 2022. snažni meteotsunamiji pogodili su nekoliko lokacija na Mediteranu, međusobno udaljenih do 500 km. Tijekom jutarnjih sati 24. svibnja 2021. meteotsunami je pogodio Bonifacio na otoku Korzici (zapadni Mediteran, Francuska), dok je poslijepodne istog dana drugi meteotsunami pogodio oko 500 km udaljeni zaljev Široka na otoku Istu (Jadransko more, Hrvatska). Otprilike 13 mjeseci kasnije, 26. lipnja 2022., meteotsunami je pogodio Ciutadellu na otoku Menorca (Španjolska) te dva dana kasnije 400 km udaljeni Bonifacio na Korzici. Detaljno su analizirana mjerenja razine mora i tlaka zraka, satelitske snimke te sinoptički uvjeti tijekom oba događaja. Potvrđeno je da se mediteranski meteorološki tsunamiji javljaju za vrijeme povoljnih sinoptičkih uvjeta – snažna jugozapadna mlazna struja unutar dinamičkih ili konvektivno nestabilnih atmosferskih slojeva prepoznata je kao najvažniji uvjet. Potencijal za nastanak meteotsunamija određen je za sva tri zaljeva (Ciutadella, Bonifacio, Široka) na temelju: (1) procjene potencijala za Proudmanovu rezonanciju na morskim pojasevima ispred zaljeva, (2) orijentacije ulaza u zaljev i (3) učestalosti sinoptičkih uvjeta povoljnih za nastanak meteoroloških tsunamija. Najjači i najučestaliji meteorološki tsunamiji javljaju se na lokacijama na kojima karakteristike morskog pojasa (širina, dubina, orijentacija), orijentacija ulaza u zaljev i distribucija povoljnih sinoptičkih uvjeta, imaju karakteristike koje pogoduju amplifikaciji dugih valova otvorenog mora te njihovom širenju prema zaljevu.

Ključne riječi: meteotsunami, Sredozemno more, Jadransko more, ekstremne razine mora, visoko-frekventne oscilacije razine mora, Proudmanova rezonancija

Corresponding author's address: Krešimir Ruić, Faculty of Science, University of Split, Ruđera Boškovića 33, 21000 Split, Croatia; tel: +381 21 619 310; e-mail: kruic@pmfst.hr

Appendix

Table A1. Date, height and literature source of the known Ciutadella, Bonifacio and Široka Bay meteotsunamis (marked in Fig. 13).

Ciutadella		
Date, hour	Height (cm)	Source
15 August 1996, 12:00	90	Šepić et al., 2009a, based on PRETLAST-96 experiment
18 June 1997, 12:00	100	Šepić et al., 2009a, based on LAST-97 experiment
4 July 1997, 12:00	125	Monserrat et al., 1998
14 July 1997, 12:00	100	Šepić et al., 2009a
23 July 1997, 12:00	125	Monserrat et al., 1998
14 July 1998, 09:00	100	Šepić et al., 2009a, based on POSTLAST-98 experiment
31 July 1998, 08:00	200	Monserrat et al., 2006
02 August 1998, 12:00	140	Šepić et al., 2009a, based on POSTLAST-98 experiment
03 August 1998, 12:00	230	Šepić et al., 2009a, based on POSTLAST-98 experiment
15 June 2006, 18:00	500	Jansà et al., 2007; Vilibić et al., 2008
23 June 2014, 23:00	100	Šepić et al., 2015a
17 July 2018, 12:00	150	https://ib3.org/rissaga-de-mes-dun-metre-a-ciutadella
18 June 2021, 12:00	120	https://www.news.de/panorama/855924085/rissaga-im-juni-2021-auf-menorca-meteo-tsunami-im-mittel-meer-meeresspiegelschwankungen-in-ciutadella/1/
16 September 2021, 16:00	118	https://www.menorca.info/menorca/sucesos/2021/09/16/1664892/ciutadella-registra-rissaga-metros.html
26 June 2022, 12:00	95	This manuscript
Bonifacio		
24 May 2021, 09:00	~100	This manuscript
28 June 2022	~100	This manuscript
Široka Bay		
22 August 2007, 17:30	~400	Šepić et al., 2009b
24 May 2021, 15:30	~300	This manuscript